ACS APPLIED MATERIALS & INTERFACES

Research Article

www.acsami.org

# Self-Assembly Formation of Lipid Bilayer Coatings on Bare Aluminum Oxide: Overcoming the Force of Interfacial Water

Joshua A. Jackman,[†,‡] Seyed R. Tabaei,[†,‡] Zhilei Zhao,[†,‡] Saziye Yorulmaz,[†,‡] and Nam-Joon Cho*[,†,‡,§]

[†]School of Materials Science and Engineering, Nanyang Technological University, 50 Nanyang Avenue, Singapore 639798, Singapore

[‡]Centre for Biomimetic Sensor Science, Nanyang Technological University, 50 Nanyang Drive, Singapore 637553, Singapore

[§]School of Chemical and Biomedical Engineering, Nanyang Technological University, 62 Nanyang Drive, Singapore 637459, Singapore

Supporting Information

**ABSTRACT:** Widely used in catalysis and biosensing applications, aluminum oxide has become popular for surface functionalization with biological macromolecules, including lipid bilayer coatings. However, it is difficult to form supported lipid bilayers on aluminum oxide, and current methods require covalent surface modification, which masks the interfacial properties of aluminum oxide, and/or complex fabrication techniques with specific conditions. Herein, we addressed this issue by identifying simple and robust strategies to form fluidic lipid bilayers on aluminum oxide. The fabrication of a single lipid bilayer coating was achieved by two methods, vesicle fusion under acidic conditions and solvent-assisted lipid bilayer (SALB) formation under near-physiological pH conditions. Importantly, quartz crystal microbalance with dissipation (QCM-D) monitoring measurements determined that the hydration layer of a supported lipid bilayer on aluminum oxide is appreciably thicker than that of a bilayer on silicon oxide. Fluorescence recovery after photobleaching (FRAP) analysis indicated that the diffusion coefficient of lateral lipid mobility was up to 3-fold greater on silicon oxide than on aluminum oxide. In spite of this hydrodynamic coupling, the diffusion coefficient on aluminum oxide, but not silicon oxide, was sensitive to the ionic strength condition. Extended-DLVO model calculations estimated the thermodynamics of lipid−substrate interactions on aluminum oxide and silicon oxide, and predict that the range of the repulsive hydration force is greater on aluminum oxide, which in turn leads to an increased equilibrium separation distance. Hence, while a strong hydration force likely contributes to the difficulty of bilayer fabrication on aluminum oxide, it also confers advantages by stabilizing lipid bilayers with thicker hydration layers due to confined interfacial water. Such knowledge provides the basis for improved surface functionalization strategies on aluminum oxide, underscoring the practical importance of surface hydration.

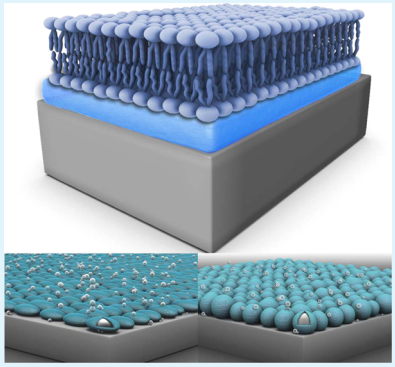

**KEYWORDS:** *surface coating, biofunctionalization, self-assembly, aluminum oxide, supported lipid bilayer, interfacial forces*

## INTRODUCTION

Phospholipid membranes on solid supports offer a two-dimensional, biocompatible thin film that is useful for applications such as biofouling-resistant coatings, biosensors, and cell culture platforms.[1−5] In particular, single lipid bilayers,[6,7] termed supported lipid bilayers, are widely explored because they mimic the fundamental properties of biological membranes, including thickness, two-dimensional fluidity, and electrical insulation, and are, in principle, suitable for hosting membrane proteins.[2,6,8] Hydrophilic solid supports offer a platform to improve the stability and lifespan of the lipid bilayer,[3] and enable characterization by surface-sensitive measurement tools.[9] For sensing applications, the intended goal of the platform is a key determinant in choosing the type of solid support, both the material composition and nanostructure. Indeed, different solid supports may have specific properties such as optical transparency (e.g., glass and indium tin oxide) or high refractive index (e.g., gold and titanium oxide). The growing numbers of applications and researchers in this field have in turn spurred efforts to develop a simple and general method to form supported lipid bilayers on hydrophilic substrates with different material compositions,[10] which is a difficult feat considering that the surface properties of individual materials vary considerably.

There are several fabrication strategies available to form supported lipid bilayers, including but not limited to Langmuir-type transfer, vesicle adsorption and rupture, bubble collapse deposition, freezing and thawing, and solvent-exchange (see refs 11 and 12, and references therein). Vesicle adsorption and rupture is the most common method and is based on the spontaneous or induced rupture of adsorbed lipid vesicles.[13,14] An adsorbed vesicle experiences shape deformation that is governed by the attractive vesicle−substrate interaction and vesicle bending energy.[15] If deformation is appreciable, then

Received: November 3, 2014
Accepted: December 16, 2014
Published: December 16, 2014

  

DOI: 10.1021/am507651h
ACS Appl. Mater. Interfaces 2015, 7, 959−968

vesicles may rupture spontaneously and lipids reassemble to form a supported lipid bilayer. Otherwise, an adsorbed vesicle will remain stably adsorbed on the substrate and not rupture unless an external trigger induces vesicle destabilization and rupture.

Intrinsically, the vesicle−substrate interaction in a particular system is largely responsible for governing the behavior of adsorbed vesicles, and the van der Waals,[16] double-layer electrostatic,[17] and hydration[18] forces have all been identified as important contributors to the adhesion energy, in turn reflecting the surface properties of the material. Experimentally, many parameters, including vesicle properties (e.g., size,[19] lipid composition,[20] lamellarity,[21] and osmotic pressure[19]), solution conditions (e.g., ionic strength,[22] temperature,[23] pH[24]), and material properties (e.g., crystallinity,[16] topology[25]), influence the vesicle−substrate adhesion energy and the magnitudes of the corresponding interfacial forces. In spite of all these parameters and the opportunities available to tune them, the outcome of vesicle adsorption is generally regarded as surface-specific,[9] leading to the formation of a saturated vesicle adlayer (e.g., on gold[8] and titanium oxide[26]) or a supported lipid bilayer (e.g., on silicon oxide[8] and mica[27]). Following this line, Groves et al.[28,29] reported that several oxide film substrates act as barriers that prevent the formation of fluidic supported lipid bilayers. Type I barriers such as aluminum oxide prevent vesicle adsorption, while Type II barriers such as indium tin oxide and chrome support vesicle adsorption but the resulting phospholipid assemblies are effectively immobile.[32]

As a hydrophilic barrier that hinders vesicle adsorption, aluminum oxide is particularly interesting because it is known[30,31] to have appreciable surface hydration in aqueous environments. The degree of surface hydration, manifested as tightly bound water molecules at the solid−liquid interface, is also known[32−34] to influence the kinetics of vesicle rupture and bilayer formation on silicon oxide. Interfacial water on aluminum oxide is reported[34,35] to be more tightly bound than on silicon oxide, suggesting that its influence on the corresponding lipid−substrate interaction may be even more significant. However, there has been limited attention to understand how interfacial water contributes to the role of aluminum oxide as a barrier to vesicle adsorption. Rather, fabrication efforts have mainly attempted to overcome the concomitantly weak adhesion energy by incorporating a vesicle-destabilizing agent (e.g., polyethylene glycol,[35] AH peptide[36]) or by chemically functionalizing the aluminum oxide surface via silanization[37−40] or covalent attachment of tethered lipid anchors.[41] Additionally, Mager et al.[42] reported bilayer formation on aluminum oxide by using the bubble collapse deposition (BCD) method; however, the fabrication process is complex, a preformed sacrificial bilayer is required, and bilayers can only form in continuous patches up to 200 $\mu$m diameter. Venkatesan et al.[43] reported that a perfusion of high ionic strength aqueous solution could induce the rupture of already adsorbed, large vesicles via osmotic stress. These studies indicate that the formation of supported lipid bilayers on aluminum oxide is possible, and provide motivation to develop simple and general strategies to form lipid bilayer coatings on aluminum oxide. Indeed, as remarked above, vesicle adsorption onto aluminum oxide is itself challenging to perform under conventional experimental conditions.

One strategy of this kind calls for increasing the vesicle−substrate adhesion energy on aluminum oxide. Like other oxide surfaces, aluminum oxide possesses surface hydroxyl groups that have a varying degree of ionization depending on environmental conditions.[44] In turn, the surface charge will vary and accordingly influence the vesicle−substrate interaction. By changing solution pH, Cho et al.[45] reported the spontaneous formation of a supported lipid bilayer on titanium oxide. At neutral pH condition, vesicles adsorb and remain intact because there is electrostatic repulsion, whereas vesicles rupture to form a supported lipid bilayer in acidic pH conditions due to electrostatic attraction. The reverse situation is also possible, with basic pH conditions inhibiting the formation of a supported lipid bilayer on silicon oxide.[46] These findings support that a similar approach may be advantageous to explore in the case of aluminum oxide.

Moreover, alternative fabrication techniques based on solvent-exchange bypass the requirements for vesicle preparation and high adhesion energy. In this case, lipids dispersed in alcohol are deposited on a solid support followed by solvent-exchange with aqueous solution in order to promote a series of phase transitions with increasing water fraction that leads to the formation of a supported lipid bilayer.[47] Using this solvent-assisted lipid bilayer (SALB) approach, Tabaei et al.[48] reported the formation of a supported lipid bilayer on gold that is generally intractable to bilayer formation via conventional vesicle fusion (see also, e.g., refs 49−51 for reports describing bilayer formation on atomically flat gold). Interestingly, the hydration mass for a supported lipid bilayer on gold was measured to be greater than for a bilayer on silicon oxide, which suggests that surface hydration inhibits vesicle rupture on gold. Similar reasoning has been offered to explain the case of titanium oxide,[18] and primarily supported by extended-DLVO model calculations which indicate that the hydration force is a governing parameter to influence the lipid−substrate interaction on titanium oxide. Clarifying the role of surface hydration in bilayer fabrication on aluminum oxide is important because the substrate, unlike silicon oxide and gold, is a barrier to vesicle adsorption. Developing simple fabrication strategies to overcome this challenge while preserving the interfacial properties of aluminum oxide would provide not only a means to functionalize bare aluminum oxide with a high-sealing, biocompatible surface coating but also offer guidelines to control noncovalent adsorption of biological macromolecules onto highly hydrated surfaces in general.

In this work, we investigated the formation of supported lipid bilayers on aluminum oxide by the vesicle fusion and SALB methods. Using quartz crystal microbalance with dissipation (QCM-D) monitoring and fluorescence recovery after photobleaching (FRAP), the mass and fluidic properties of supported lipid bilayers on aluminum oxide are characterized. The measurements are complemented by extended-DLVO model calculations which estimate the predicted equilibrium separation distance between the supported lipid bilayer and substrate as well as the corresponding thermodynamics of the system. Taken together, the findings help to understand how the interfacial forces influence lipid−substrate interactions and outline an approach to spontaneously form lipid bilayer coatings on surfaces with high surface hydration.

## MATERIALS AND METHODS

**Vesicle Preparation.** Small unilamellar vesicles composed of 1-palmitoyl-2-oleoyl-*sn*-glycero-3-phosphocholine (POPC) lipid (Avanti Polar Lipids, Alabaster, AL) were prepared by the extrusion method as previously described.[52] First, dried lipid films were prepared by drying as-received lipids in chloroform with nitrogen air. After storage in a


DOI: 10.1021/am507651h
ACS Appl. Mater. Interfaces 2015, 7, 959−968

vacuum desiccator for 24 h, the lipid film was hydrated at a nominal lipid concentration of 5 mg/mL in a 10 mM Tris [pH 7.5] buffer solution with 150 mM NaCl, followed by vortexing to form large multilamellar vesicles. The vesicles were then passsed 17 times through a miniextruder (Avanti Polar Lipids), with a track-etched polycarbonate membrane of 100 nm diameter pore size. Similar extrusion cycles were subsequently performed with membranes of 50 and 30 nm pore sizes. Following extrusion, the resulting small unilamellar vesicles were diluted in Tris buffer solution of appropriate pH to 0.125 mg/mL concentration. Tris buffer solutions of varying pH were prepared via titration with 1 M hydrochloric acid (HCl) and/or 1 M sodium hydroxide (NaOH). Before experiment, the solution pH was verified and adjusted, if necessary. All buffer solutions were prepared with Milli-Q-treated water (resistivity > 18.2 MΩ·cm) (Millipore, Billerica, MA).

**Lipid Solution for SALB Experiments.** POPC lipid powder (Avanti Polar Lipids) was dissolved immediately before experiment in isopropyl alcohol at a 10 mg/mL lipid concentration and then diluted to the final lipid concentration of 0.5 mg/mL. For fluorescence microscopy experiments, 0.5 wt % 1,2-dioleoyl-*sn*-glycero-3-phosphoethanolamine-*N*-(lissamine rhodamine B sulfonyl) (ammonium salt) (Rhodamine-DOPE) lipid was added to the mixture.

**Dynamic Light Scattering.** The size distribution of extruded vesicles in solution was determined by using a 90Plus particle size analyzer (Brookhaven Instruments, Holtsville, NY) that has a 658 nm monochromatic laser. To minimize the reflection effect, the scattering angle was set at 90°. Temporal fluctuations in the intensity of scattered light were recorded and analyzed by the cumulants method in order to calculate the size distribution of vesicles. The average diameter of vesicles reported in this work was 60.3 nm with a polydispersity of 0.054, as presented in Figure S1 (Supporting Information).

**Quartz Crystal Microbalance with Dissipation (QCM-D) Monitoring.** A Q-Sense E4 instrument (Q-Sense AB, Gothenburg, Sweden) was used to track adsorption processes by monitoring changes in resonance frequency and energy dissipation as functions of time.[53] The temperature of the measurement cell was 25.0 ± 0.5 °C. All measurements were performed on 14 mm diameter, 5 MHz quartz crystals (Q-Sense AB) with sputter-coated silicon oxide (model no. QSX303) or aluminum oxide (model no. QSX309) surface coatings. The quartz crystals have a mass sensitivity of 17.7 ng/cm$^2$ per 1 Hz. Prior to experiment, each sensor crystal was treated with oxygen plasma at maximum radiofrequency power for 5 min (Harrick Plasma, Ithaca, NY), and the aluminum oxide-coated substrates had a contact angle of 38 ± 2° and a root-mean-square surface roughness of 1.2 ± 0.8 nm. Data was collected at the $n$ = 3, 5, and 7 odd overtones, and normalized according to the overtone number. All data presented in Figures 1 and 2 and Table 1 were obtained at the third overtone. Data analysis was performed using the Sauerbrey and Voigt-Voinova models,[54] as available in the QTools software package. For the Voigt-Voinova model fitting, the effective film thickness of an adsorbed vesicle layer was calculated by assuming the film density to be 1000 kg/m$^3$ and the viscosity of the bulk aqueous solution to be 0.001 Pa/s. For all experiments, liquid sample was added under continuous flow at a rate of 50 μL/min, as regulated by a Reglo Digital peristaltic pump (Ismatec, Glattbrugg, Switzerland).

**Epifluorescence Microscopy.** Experiments were conducted using an inverted epifluorescence Eclipse TE 2000 microscope (Nikon) equipped with a 60× oil immersion objective (NA 1.49), and an Andor iXon+ EMCCD camera (Andor Technology, Belfast, Northern Ireland). A mercury lamp (Intensilight C-HGFIE; Nikon Corporation) was used to illuminate samples through a TRITC (rhodamine–DOPE) filter set. The acquired images consisted of 512 × 512 pixels with a pixel size of 0.267 × 0.267 μm. For FRAP measurements, a 30 μm-wide circular spot was photobleached with a 532 nm, 100 mW laser and diffusion coefficients were computed by the Hankel transform method.[55] For experiments on glass, standard glass coverslips (Menzel Gläser, Braunschweig, Germany) attached to a stick-Slide I0.1 microfluidic flow cell (Luer, Ibidi, Munich, Germany) were used. For experiments on aluminum oxide, a similar setup was employed using sputtered aluminum oxide thin films (10 nm thickness) that were prepared on a glass substrate by reactive RF-magnetron sputtering at a power of 100 W.

**Ellipsometry.** The thickness of lipid layers on aluminum oxide-coated substrates was measured using a Nanofilm EP3 ellipsometer (Accurion GmbH, Germany) with the EP3View software package. Incident light with a wavelength of 545.6 nm was selected from a xenon lamp by using an interference filter, and the angle of incidence was 65°. The measured Δ and Ψ signals were fit to a layered structure in order to determine the complex refractive index and thickness of each layer by using the EP4Model software (Accurion GmbH). To obtain the optical properties of the substrates, measurements were conducted in water ($n$ = 1.333), buffer ($n$ = 1.335), and isopropyl alcohol ($n$ = 1.378). Lipid layers deposited on the substrate were modeled as a homogeneous adlayer with a refractive index $n$ and a thickness $d$.[56] $n$ was constrained from 1.33 (refractive index of water) to 1.5 (refractive index of a lipid bilayer), and $d$ was constrained from 0 to 100 nm. The optical mass of the layer, $\Delta m_{optical}$, was determined from $n_{layer}$ and $d_{layer}$ by using the de Feijter[57] formula with a $dn/dc$ value of 0.13 mL/g for the refractive index increment.

**Contact Angle Measurements.** Static contact angle measurements were performed on oxygen plasma-treated aluminum oxide substrates with an Attension Theta Optical Tensiometer (Biolin Scientific, Stockholm, Sweden). A constant droplet volume of 4 μL Milli-Q-treated water was used.

## RESULTS AND DISCUSSION

**Effect of Solution pH on Vesicle Adsorption.** We first investigated the adsorption kinetics of 60 nm diameter POPC lipid vesicles onto an aluminum oxide-coated quartz crystal as a function of solution pH by using the QCM-D measurement technique. With decreasing solution pH, it has been reported that zwitterionic lipid vesicles have more attractive vesicle–substrate interactions on titanium oxide and silicon oxide film surfaces.[46] Changes in frequency and energy dissipation of an oscillating quartz crystal are tracked as a function of time and provide information about the mass and viscoelastic properties of an adsorbate, respectively (see, e.g., ref 10, and references therein). For a supported lipid bilayer, typical frequency and energy dissipation shifts are around −26 Hz and below 0.5 × $10^{-6}$, respectively. By contrast, for a saturated vesicle adlayer, typical frequency and energy dissipation shifts are greater than −100 Hz and 6 × $10^{-6}$, respectively. A baseline recording was obtained in the desired aqueous solution (without vesicle), and then vesicles in an equivalent solution were added at $t$ = 1 min. The corresponding frequency and energy dissipation shifts were due to vesicle adsorption onto the substrate. At pH 8, there was monotonic adsorption of lipid vesicles leading to changes in frequency and energy dissipation of −32 Hz and 2.2 × $10^{-6}$, respectively (Figure 1A). These values are well below the typical values for saturation of adsorbed vesicles,[19] indicating that vesicle adsorption is minimal in this case. The same experiment was performed at pH 8.5, and no adsorption was observed (Figure S2, Supporting Information). These results are consistent with aluminum oxide acting as a barrier that prevents vesicle adsorption in this pH range.[25,26]

By contrast, with decreasing solution pH, vesicle adsorption onto aluminum oxide increased appreciably. At pH 6, there was significant vesicle adsorption with maximum changes in frequency and energy dissipation of −126 Hz and 8.7 × $10^{-6}$, respectively (Figure 1B). However, the vesicle configuration on the substrate was not stable and there was a change in the physical properties of the adlayer during the adsorption process, as evidenced by the positive increase in the frequency signal and corresponding decrease in the energy dissipation signal. These measurement responses are consistent with a


DOI: 10.1021/am507651h
ACS Appl. Mater. Interfaces 2015, 7, 959–968

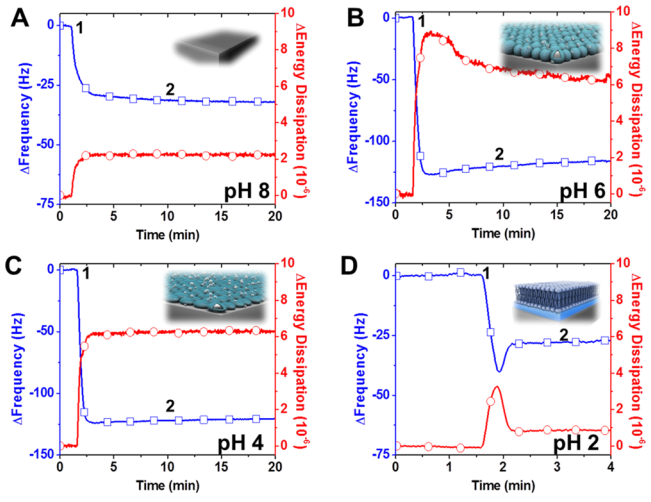


**Figure 1.** QCM-D monitoring of vesicle adsorption onto aluminum oxide. Changes in frequency (blue squares) and energy dissipation (red circles) were recorded as a function of time. The measurement baseline was recorded in aqueous buffer solution. Lipid vesicles were added at approximately $t$ = 1 min and the adsorption studies were performed in different solution pH conditions as follows: (A) pH 8, (B) pH 6, (C) pH 4, and (D) pH 2. Labels 1 and 2 indicate vesicle addition and buffer wash, respectively.

decrease in the surface coverage of adsorbed vesicles.[18] Within 15 min, the final changes in frequency and energy dissipation had reached −116 Hz and 6.3 × $10^{-6}$, respectively. In the pH range of 4−5, irreversibly adsorbed vesicle layers were formed. At pH 4, the changes in frequency and energy dissipation were −121 Hz and 6.3 × $10^{-6}$, respectively (Figure 1C). Similar results were also obtained at pH 5 (Figure S3, Supporting Information). Importantly, Voigt−Voinova model analysis indicated that the effective film thickness of the vesicle adlayer at pH 5 was greater than at pH 4 (40 nm vs 32 nm at pH 5 and 4, respectively; see Figure S4, Supporting Information). These values support that, with decreasing solution pH, vesicle deformation becomes more appreciable, indicating that vesicle−substrate interactions are increasingly attractive. Notably, the extent of vesicle deformation on aluminum oxide in this pH range is less than previously measured by Schönherr et al.[15] for similar-size vesicles on silicon oxide under pH 8 solution conditions (i.e., a regime in which vesicles rupture after reaching a critical vesicle coverage). Hence, the adsorbed vesicles on aluminum oxide are deformed but the extent of deformation is insufficient to cause spontaneous rupture.

Therefore, we reasoned that more appreciable vesicle deformation, brought on by a stronger vesicle−substrate interaction, must occur in order to promote vesicle rupture on aluminum oxide. At pH 2, vesicle adsorption led to rupture after reaching a critical coverage (Figure 1D). Upon adsorption, the critical coverage was identified based on changes in frequency and energy dissipation of −40 Hz and 3.0 × $10^{-6}$, respectively. Afterward, vesicles began to rupture and the final changes in frequency and energy dissipation were −27 Hz and 0.8 × $10^{-6}$, respectively. The frequency shift is consistent with bilayer formation (4.8 nm thickness according to the Sauerbrey equation[58]), whereas the energy dissipation is somewhat higher than that typically observed for supported lipid bilayers on silicon oxide (less than 0.5 × $10^{-6}$ is preferable[10]). Although one possible explanation is the presence of a fraction of unruptured vesicles, the difference could also be attributed to greater surface hydration for a supported lipid bilayer on aluminum oxide.

**Bilayer Fabrication by the SALB Procedure.** To further investigate the formation of supported lipid bilayers on aluminum oxide, we used the SALB formation method. As described in the Introduction, this method does not require vesicles. It is instead based on solvent-assisted lipid self-assembly when lipids in alcohol are deposited on a substrate and then solvent-exchange is performed leading to an increase in the water fraction. As the water fraction increases, lipids attached to the surface and in solution undergo a series of phase transitions eventually forming a supported lipid bilayer. Notably, the adhesion energy needed to stabilize a supported lipid bilayer on aluminum oxide is likely much less than that required for adsorbed vesicles to rupture,[42] and the SALB procedure therefore offers a solution to bypass the high contact energy requirements of vesicle rupture. Hence, we attempted to form a supported lipid bilayer at pH 7.5 via the SALB procedure. Figure 2 presents representative QCM-D measurement traces for SALB experiments on aluminum oxide. Similar experiments were also performed on silicon oxide for comparison.

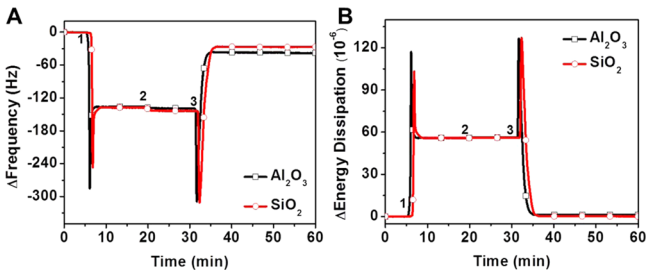


**Figure 2.** QCM-D monitoring of supported lipid bilayer formation via the SALB procedure. Change in QCM-D (A) frequency and (B) energy dissipation signal as a function of time are presented throughout the entire process. The measurement baseline was recorded in aqueous buffer solution, followed by solvent-exchange with isopropyl alcohol (label 1), addition of 0.5 mg/mL POPC lipid in isopropyl alcohol solution (label 2), and solvent-exchange returning to aqueous buffer solution (label 3).

A measurement baseline was first recorded in aqueous buffer solution (10 mM Tris buffer [pH 7.5] with 150 mM NaCl), followed by exchange with isopropyl alcohol solution at $t$ = 5 min. Afterward, 0.5 mg/mL POPC lipid in isopropyl alcohol was deposited onto the substrate at $t$ = 20 min, and lipid attachment reached equilibrium. On aluminum oxide, lipid attachment in isopropyl alcohol corresponded to a −3.8 ± 1.1 Hz frequency shift. By contrast, on silicon oxide, lipid attachment resulted in a −5.9 ± 0.3 Hz frequency shift, which indicates a greater amount of attached lipid to silicon oxide.

After lipid attachment in isopropyl alcohol, a solvent-exchange step was performed at $t$ = 30 min in order to reintroduce aqueous solution (without lipid) and complete the SALB procedure. The final frequency and dissipation shifts are reported in Table 1. On aluminum oxide, the final frequency and energy dissipation shifts were −37.5 ± 0.7 Hz and 1.2 ± 0.3 × $10^{-6}$, respectively. By contrast, on silicon oxide, the final frequency and energy dissipation shifts were −26.2 ± 0.6 Hz and 0.3 ± 0.1 × $10^{-6}$, respectively, which are in agreement with


DOI: 10.1021/am507651h
ACS Appl. Mater. Interfaces 2015, 7, 959−968

**Table 1. QCM-D Measurement Responses Obtained for Supported Lipid Bilayers Formed via the SALB Procedure[a]**

| substrate | lipid adsorption (Hz) | final frequency (Hz) | final dissipation ($10^{-6}$) |
|---|---|---|---|
| aluminum oxide | −3.8 ± 1.1 | −37.5 ± 0.7 | 1.2 ± 0.3 |
| silicon oxide | −5.9 ± 0.3 | −26.2 ± 0.6 | 0.3 ± 0.1 |

[a]The frequency shift associated with lipid adsorption in isopropyl alcohol solution onto the solid support is reported along with the final frequency and energy dissipation values for supported lipid bilayers in aqueous solution after completion of the SALB experimental procedure. The average and standard deviation of each measurement value are reported for $n$ = 3 independent experiments per substrate.

past measurements.[48] To determine if the lipid layer on aluminum oxide was globally homogeneous, we measured the nonspecific adsorption of bovine serum albumin, which was nearly negligible (~1 Hz). By contrast, BSA adsorption onto a bare aluminum oxide surface yielded a frequency shift of approximately −28 Hz, and we conclude that the attached lipid layer covers more than 96% of the aluminum oxide substrate (Figure S5, Supporting Information). Furthermore, the optical mass density of the lipid layer on aluminum oxide was determined by ellipsometric measurements to be around 400 ng/cm$^2$, which is consistent with a single lipid bilayer coating[36] (Figure S6, Supporting Information).

In light of these considerations, one possible explanation for the difference in measurement values on the two substrates is a thicker hydration layer on aluminum oxide. Let us assume that the difference in the frequency shifts between the aluminum oxide and silicon oxide cases is due to coupled solvent in the hydration layer and that the density of this solvent is equivalent to liquid water (1 g/cm$^3$). By applying the Sauerbrey relationship,[58] we estimate that a 1 Hz shift deviation is due to a 0.177 nm thicker hydration layer. The hydration layer for a supported lipid bilayer on aluminum oxide would be ~2.1 nm thicker (~12 Hz shift difference) than on silicon oxide. This estimated range is consistent with previous atomic force microscopy (AFM) thickness measurements for supported lipid bilayers on aluminum oxide[43] (~6.5 nm) and silicon oxide[59] (~4.6 nm) with similar chain-length lipids under nearly equivalent pH conditions. Taken together, the QCM-D measurement values and supporting data indicate that a supported lipid bilayer is formed on aluminum oxide by using the SALB approach. The difference in the frequency shifts for supported lipid bilayers formed on aluminum oxide by the two methods is likely due to variation in the strength of the lipid−substrate interaction under acidic versus near-neutral pH conditions. As the SALB procedure directly yields a supported lipid bilayer on aluminum oxide under biologically relevant pH conditions, it is likely the more favorable method for widespread application and was therefore subjected to more detailed characterization efforts.

**FRAP Analysis of Supported Lipid Bilayer on Aluminum Oxide.** To further investigate the fluidic properties of supported lipid bilayers formed by the SALB procedure, we performed FRAP measurements. For these experiments, 0.5 wt % fluorescently labeled Rhodamine-DOPE lipid was included in the precursor mixture in isopropyl alcohol in order to visualize the supported lipid bilayers. After completion of the SALB procedure, the ionic strength of the solution was varied by titration and FRAP measurements were recorded at each ionic strength condition. Lateral lipid diffusion was observed for the supported lipid bilayer on aluminum oxide, as indicated in representative FRAP snapshots presented in Figure 3A. At 100 mM ionic strength, the diffusion coefficient of the supported lipid bilayer on aluminum oxide was 0.76 ± 0.19 $\mu$m$^2$/s, which is in agreement with previous diffusion coefficients[42] (0.62 ± 0.21 $\mu$m$^2$/s) obtained for lipid bilayer patches on aluminum oxide formed by the BCD method under nearly identical ionic strength and pH conditions. Figure 3B presents normalized fluorescence intensity traces of the bleached spot and the mobile fraction was ~86%, which is also in agreement with previous measurements.[42] The calculated diffusion coefficient and mobile fraction are lower than those which are typically obtained on silicon oxide,[42] and this difference has been attributed to stronger hydrodynamic coupling. Previous NMR studies on oxide nanoparticles also indicate that water near an

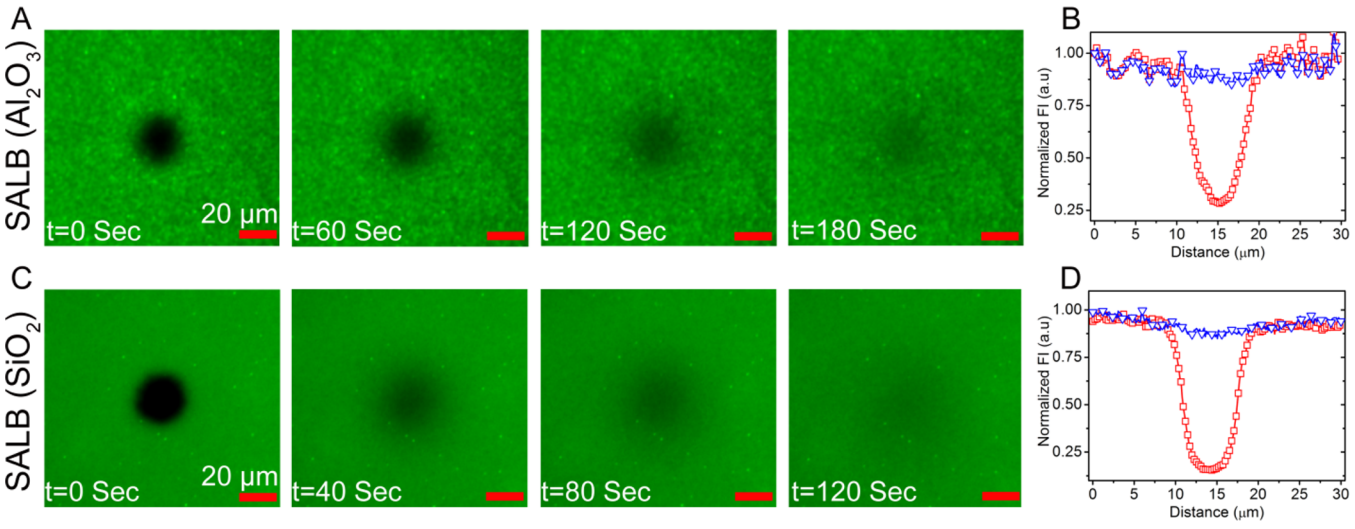


**Figure 3.** Observation of fluidic lipid bilayers on aluminum oxide. (A) Time-lapsed fluorescence micrographs are presented for a supported lipid bilayer on aluminum oxide formed via the SALB procedure. The dark spot in the image center corresponds to the bleached spot. (B) Normalized intensity profiles of the bleached spot on aluminum oxide before (red squares) and after recovery (blue circles). Panels C and D present similar results obtained for a supported lipid bilayer on silicon oxide formed via the SALB procedure. In Panels A and C, the scale bars are 20 $\mu$m.



DOI: 10.1021/am507651h
ACS Appl. Mater. Interfaces 2015, 7, 959−968

aluminum oxide surface is less mobile than that near a silicon oxide surface.[30,31] By contrast, at 100 mM ionic strength, the diffusion coefficient and mobile fraction of the supported lipid bilayer on silicon oxide are 2.28 ± 0.15 $\mu m^2/s$ and >90%, which are in agreement with literature values[7,60,61] (Figure 3C,D).

On both substrates, the FRAP measurement results are also reported as a function of ionic strength by varying the NaCl concentration (Figure 4). For aluminum oxide, the diffusion coefficient increased with increasing ionic strength along with the mobile fraction (>90%). At 50 mM NaCl, the diffusion coefficient was 0.70 ± 0.20 $\mu m^2/s$, whereas it increased to 1.43 ± 0.20 $\mu m^2/s$ at 1000 mM NaCl. Hence, depending on the ionic strength, the diffusion coefficient varied by up to 2-fold and the trend is consistent with the high diffusion coefficient reported by Venkatesan et al.[43] for a supported lipid bilayer on aluminum oxide under similar high salt conditions (10 mM Tris buffer [pH 8.0] with 1000 mM KCl and 5 mM $CaCl_2$). By contrast, on silicon oxide, the diffusion coefficient of a supported lipid bilayer was largely independent of the ionic strength, maintaining a value around 2.4 $\mu m^2/s$. Although the specific contributions of ions to the hydration force are complex and multifactorial,[62] the different effects of changing ionic strength for bilayers on the two substrates observed here suggest that ionic strength influences properties of the hydration layer which couples the bilayer to the substrate, rather than the lipid bilayer itself. That is, the properties of the hydration layer for supported lipid bilayers on the two substrates appear to vary and strongly influence the fluidic properties of the lipid bilayer. In part, variation in the hydration layers on the two substrates is evident from the different layer thicknesses, and the thicker layer of confined interfacial water molecules in the aluminum oxide system appears to confer a greater response to environmental stimuli (e.g., ionic strength perturbations).

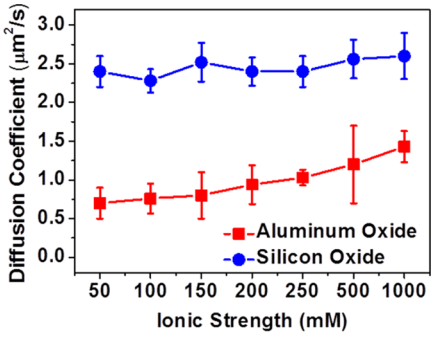


**Figure 4.** FRAP analysis of supported lipid bilayers as a function of ionic strength. Diffusion coefficient of lateral lipid mobility is presented as a function of ionic strength by varying the NaCl concentration. Reference measurements were also made for a supported lipid bilayer on silicon oxide. The average and standard deviation of each value are reported for $n$ = 5 measurements.

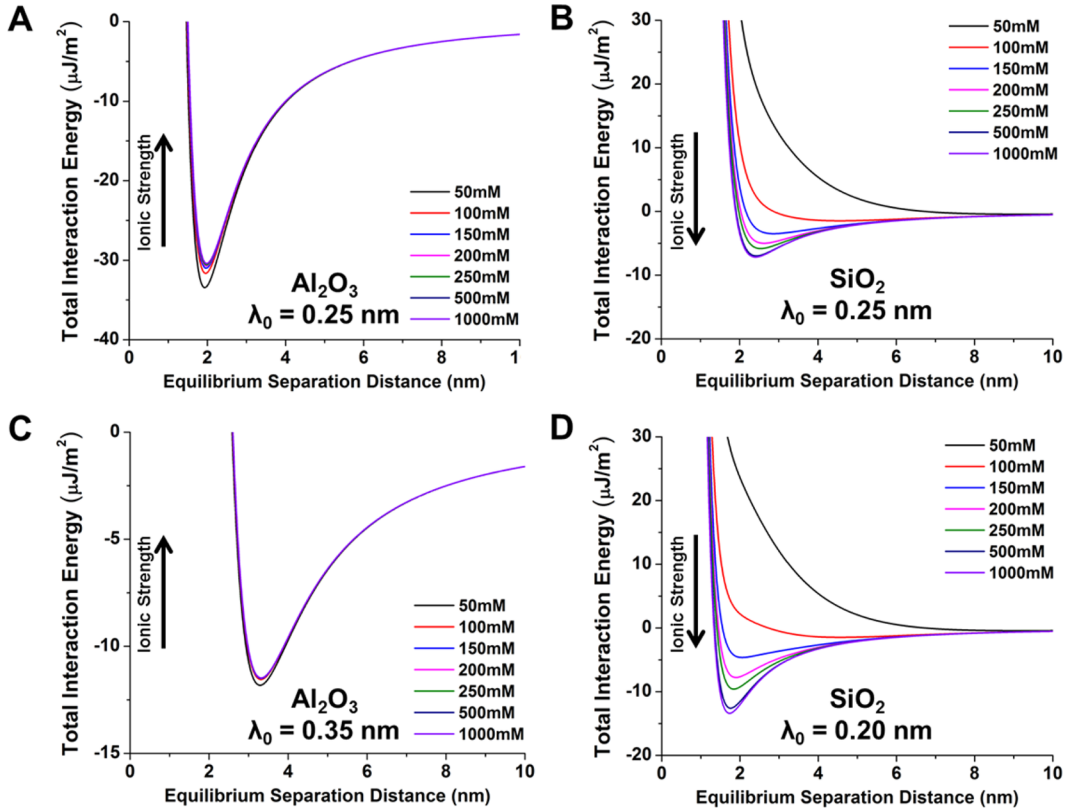


**Figure 5.** Total interaction energy of lipid−substrate interactions on solid supports. Total interaction energy as a function of separation distance between a supported lipid bilayer and aluminum oxide or silicon oxide was estimated based on extended-DLVO theory. In the model calculations, different values corresponding to the decay length of the hydration force were tested, including 0.25 nm on (A) aluminum oxide and (B) silicon oxide. Additional plots are presented for (C) 0.35 nm decay length on aluminum oxide, and (D) 0.20 nm decay length on silicon oxide. The graphs presented do not show the short-range, attractive interaction which typically occurs at separation distances below 0.3 nm. The arrows (labeled ionic strength) in each panel depict the trend in the total interaction energy with increasing ionic strength.


DOI: 10.1021/am507651h
ACS Appl. Mater. Interfaces 2015, 7, 959−968

**Extended-DLVO Model Analysis of Lipid−Substrate Interaction.** The hydration layer between the supported lipid bilayer and the substrate can also be viewed as the cumulative effect of the forces stabilizing the system. From this viewpoint, the bilayer and substrate are treated as two parallel planes and the equilibrium separation distance (i.e., hydration layer thickness) corresponding to the minimum total interaction energy between the two planes is calculated. In our approach, we use an extended DLVO-type model[16,18,63−66] that takes into account the van der Waals, double-layer electrostatic, and hydration forces. The details of the calculations are provided in the Supporting Information (Table S1 and Figure S7−S9; see ref 18), and we primarily focus here on treatment of the hydration force and its corresponding effect on the total interaction energy. The hydration force is a short-range repulsive force between two hydrophilic surfaces and may be represented as an exponential decay function with a characteristic decay length, $\lambda_0$, that describes the range of the hydration interaction energy.[67,68]

We have two primary motivations for scrutinizing the hydration force. First, in the vesicle adsorption experiments (see Figure 1), we varied the solution pH and observed the effect on vesicle adsorption. In previous work,[45] it was discussed that changing the solution pH can lead to vesicle rupture and bilayer formation on titanium oxide under conditions of electrostatic attraction between vesicles and the substrate. For the present experiments, the isoelectric point of the aluminum oxide coating is 8.7 ± 0.4[69] (the generally reported value[70] is 8.8). Below this pH value, the substrate has a positive charge while the vesicles remain negatively charged.[45] Nevertheless, vesicles adsorb and do not rupture at pH 4 or 6 when there is electrostatic attraction. Hence, the experimental findings support that an attractive electrostatic force is insufficient for vesicle rupture and suggest that solution pH also affects either the van der Waals force or hydration force. The van der Waals force is always attractive (and stronger on aluminum oxide than silicon oxide; see Figure S7, Supporting Information) and its strength is independent of the solution pH so the hydration force is likely the main factor to explain the effect of solution pH on vesicle adsorption onto aluminum oxide. Specifically, the hydration force is expected to become weaker with decreasing solution pH in order to facilitate a stronger lipid−substrate interaction. Second, the QCM-D measurement values from the SALB experiments show that the supported lipid bilayer on aluminum oxide has a relatively thicker hydration layer under near-neutral pH conditions, which is due to confined interfacial water indicative of a strong hydration force. By contrast, the relatively smaller frequency shift observed for a supported lipid bilayer formed via vesicle fusion under acidic conditions (cf Figure 1D) is likely due to a thinner hydration layer and correspondingly more attractive lipid−substrate interaction energy as compared to the bilayer formed by the SALB procedure. To facilitate a quantitative analysis of the hydration force in this context, we compare the interaction energies of supported lipid bilayers formed on aluminum oxide and silicon oxide.

In Figure 5, the total interaction energy as a function of separation distance is presented for supported lipid bilayers on aluminum oxide or silicon oxide at varying decay lengths of the hydration force. In our calculations, we treated the decay length as the free parameter and initially assume that the supported lipid bilayer has an equivalent hydration force on the two substrates. At 0.25 nm decay length (in the range cited in past works for lipid bilayers on silicon oxide[63,64]), we observe that the equilibrium separation distance for a supported lipid bilayer on aluminum oxide is predicted to be 1.97 nm and the corresponding total interaction energy decreases with increasing ionic strength from −36 to −29 $\mu J/m^2$ (Figure 5A). By contrast, on silicon oxide, a supported lipid bilayer is predicted to have an equilibrium separation distance of 2.41 nm at high ionic strength and the corresponding total interaction energy is around −7 $\mu J/m^2$ (Figure 5B). Under low ionic strength conditions, the lipid−substrate interaction is predicted to be energetically unfavorable. From these results, one would predict that a supported lipid bilayer on silicon oxide has a greater separation distance than a bilayer on aluminum oxide. However, this prediction is not consistent with the experimental evidence (obtained in this study and other reports[43]), suggesting that the assumption that the decay lengths of the hydration force on the two substrates are equivalent is invalid. Rather, it appears that the decay length of the hydration force varies on the two substrates.

Motivated by these preliminary conclusions, we refined our calculations in order to be more consistent with experimental measurements of the bilayer thickness (i.e., 2 nm thicker on aluminum oxide than on silicon oxide, which is attributed to confined interfacial water). To do so, we selected decay lengths that provide experimentally reasonable estimates of the equilibrium separation distance. In particular, the total interaction energy for a supported lipid bilayer on aluminum oxide was estimated for a decay length of 0.35 nm, yielding an equilibrium separation distance of 3.33 nm and a total interaction energy around −13 $\mu J/m^2$ (Figure 5C). The separation distance is compatible with the expected hydration layer thickness on aluminum oxide films based on our QCM-D measurement results. Likewise, for a supported lipid bilayer on silicon oxide, a decay length of 0.20 nm was used and a separation distance of 1.73 nm is predicted along with a total interaction energy around −13 $\mu J/m^2$ (Figure 5D). Taken together, the extended-DLVO model calculations demonstrate that the range of the hydration force for a supported lipid bilayer on aluminum oxide is appreciably greater than for a lipid bilayer on silicon oxide.

Furthermore, the observed dependence on ionic strength in the model calculations offers another interesting insight. On aluminum oxide, the magnitude of the total interaction energy at the equilibrium separation distance weakly decreased with increasing ionic strength because the double-layer electrostatic force is nearly negligible under the experimental conditions. In this case, stabilization of a supported lipid bilayer on aluminum oxide is principally due to the balance between the attractive van der Waals force (which decreases with increasing ionic strength) and the repulsive hydration force. By contrast, on silicon oxide, the magnitude of the total interaction energy at the equilibrium separation distance strongly increased with increasing ionic strength. In this case, the double-layer electrostatic force is strongly repulsive and stabilization is due to all three forces (the electrostatic force decreases with increasing strength due to shielding effects). Hence, the balance of interfacial forces can vary considerably depending on the substrate and may help to explain why the dependence of the lateral lipid mobility on ionic strength showed different trends on the two substrates in this study.

In summary, the extended-DLVO model calculations support that the hydration force for a supported lipid bilayer on aluminum oxide is comparatively stronger than for a bilayer on


DOI: 10.1021/am507651h
ACS Appl. Mater. Interfaces 2015, 7, 959−968

silicon oxide. In line with recent arguments to explain the lipid−substrate interaction on titanium oxide,[18] it appears that a strong hydration force on aluminum oxide in near-neutral aqueous buffer conditions is likely involved in inhibiting the rupture of adsorbed vesicles by way of decreasing the strength of the lipid−substrate interaction. The theoretical results are consistent with our experimental findings and highlight the utility of the SALB method to fabricate lipid bilayer coatings on solid supports with high surface hydration. Indeed, while a strong hydration force increases the challenge of bilayer fabrication, it also confers possible advantages by stabilizing lipid bilayers with thicker hydration layers due to the confined interfacial water.

## CONCLUSION

In this work, we have investigated self-assembly methods to fabricate lipid bilayer coatings on aluminum oxide, in turn revealing key information about the interfacial forces at play in this system. First, we explored vesicle adsorption on the substrate. While adsorbed vesicles are known to undergo shape deformation, the contributing factors that govern the vesicle−substrate contact energy have been difficult to clarify. Importantly, the QCM-D measurements identified that deformation of adsorbed vesicles increases with decreasing pH. The trend was not consistent with electrostatic attraction being sufficient for vesicle rupture; rather, the findings point to an additional factor, the hydration force. To overcome the repulsive force of confined interfacial water, we employed the SALB approach to fabricate lipid bilayer coatings under near-physiological pH conditions. Compared to supported lipid bilayers on silicon oxide, bilayers on aluminum oxide had appreciably thicker hydration layers. FRAP measurements further support that the hydration layer on aluminum oxide is tightly coupled to the substrate and in turn leads to hydrodynamic coupling with the bilayer, as reflected in a lower diffusion coefficient in this case than for bilayers on silicon oxide. Likewise, the diffusion coefficient of a bilayer on aluminum oxide, but not silicon oxide, was affected by the ionic strength condition. Complementing the experimental observations, extended-DLVO model calculations indicate that the hydration force of a supported lipid bilayer on aluminum oxide has a much greater decay length, which means that the hydration force has a longer range, likely due to the confinement of water molecules at the interface. Consequently, the hydration force has an important steric factor that contributes to its repulsive nature by retarding the other interfacial forces, most notably the van der Waals force. As demonstrated herein, this issue can be overcome for lipids by using the SALB approach to deposit lipids in alcohol, followed by solvent-exchange to spontaneously form the supported lipid bilayer. For other types of biological macromolecules, especially those with secondary structures, such strategies may not be possible due to the risk of denaturation and highlight the importance of taking surface hydration into account for biomacromolecular adsorption in general.

## ASSOCIATED CONTENT

### Supporting Information

More information is provided about DLS measurements (Figure S1), additional QCM-D experimental results (Figures S2 and S5) and Voigt−Voinova model analysis (Figures S3 and S4), and ellipsometry measurements (Figure S6) as well as extended-DLVO model calculations (Table S1 and Figures S7−S9) This material is available free of charge via the Internet at http://pubs.acs.org/.

## AUTHOR INFORMATION

### Corresponding Author

*N.-J. Cho. E-mail: njcho@ntu.edu.sg.

### Notes

The authors declare no competing financial interest.

## ACKNOWLEDGMENTS

The authors acknowledge support from the National Research Foundation (NRF -NRFF2011-01), the National Medical Research Council (NMRC/CBRG/0005/2012), and Nanyang Technological University to N.J.C. J.A.J. is a recipient of the Nanyang President's Graduate Scholarship. The authors wish to thank Ethan Ryu and Leo Byun for technical support with QCM-D experiments.

## REFERENCES

(1) Chan, Y.-H. M.; Boxer, S. G. Model Membrane Systems and Their Applications. *Curr. Opin. Chem. Biol.* **2007**, *11*, 581−587.
(2) Sackmann, E. Supported Membranes: Scientific and Practical Applications. *Science* **1996**, *271*, 43−48.
(3) Parikh, A. N.; Groves, J. T. Materials Science of Supported Lipid Membranes. *MRS Bull.* **2006**, *31*, 507−512.
(4) Czolkos, I.; Jesorka, A.; Orwar, O. Molecular Phospholipid Films on Solid Supports. *Soft Matter* **2011**, *7*, 4562−4576.
(5) Castellana, E. T.; Cremer, P. S. Solid Supported Lipid Bilayers: From Biophysical Studies to Sensor Design. *Surf. Sci. Rep.* **2006**, *61*, 429−444.
(6) Boxer, S. G. Molecular Transport and Organization in Supported Lipid Membranes. *Curr. Opin. Chem. Biol.* **2000**, *4*, 704−709.
(7) Tamm, L. K.; McConnell, H. M. Supported Phospholipid Bilayers. *Biophys. J.* **1985**, *47*, 105−113.
(8) Keller, C.; Kasemo, B. Surface Specific Kinetics of Lipid Vesicle Adsorption Measured with a Quartz Crystal Microbalance. *Biophys. J.* **1998**, *75*, 1397−1402.
(9) Florin, E.-L.; Gaub, H. Painted Supported Lipid Membranes. *Biophys. J.* **1993**, *64*, 375−383.
(10) Cho, N.-J.; Frank, C. W.; Kasemo, B.; Höök, F. Quartz Crystal Microbalance with Dissipation Monitoring of Supported Lipid Bilayers on Various Substrates. *Nat. Protoc.* **2010**, *5*, 1096−1106.
(11) Richter, R. P.; Bérat, R.; Brisson, A. R. Formation of Solid-Supported Lipid Bilayers: An Integrated View. *Langmuir* **2006**, *22*, 3497−3505.
(12) Hardy, G. J.; Nayak, R.; Zauscher, S. Model Cell Membranes: Techniques to Form Complex Biomimetic Supported Lipid Bilayers via Vesicle Fusion. *Curr. Opin. Colloid Interface Sci.* **2013**, *18*, 448−458.
(13) Watts, T. H.; Brian, A. A.; Kappler, J. W.; Marrack, P.; McConnell, H. M. Antigen Presentation by Supported Planar Membranes Containing Affinity-Purified I-Ad. *Proc. Natl. Acad. Sci. U. S. A.* **1984**, *81*, 7564−7568.
(14) McConnell, H.; Watts, T.; Weis, R.; Brian, A. Supported Planar Membranes in Studies of Cell-Cell Recognition in the Immune System. *Biochim. Biophys. Acta* **1986**, *864*, 95−106.
(15) Schönherr, H.; Johnson, J. M.; Lenz, P.; Frank, C. W.; Boxer, S. G. Vesicle Adsorption and Lipid Bilayer Formation on Glass Studied by Atomic Force Microscopy. *Langmuir* **2004**, *20*, 11600−11606.
(16) Tero, R.; Ujihara, T.; Urisu, T. Lipid Bilayer Membrane with Atomic Step Structure: Supported Bilayer on a Step-and-Terrace $TiO_2$(100) Surface. *Langmuir* **2008**, *24*, 11567−11576.
(17) Cha, T.; Guo, A.; Zhu, X.-Y. Formation of Supported Phospholipid Bilayers on Molecular Surfaces: Role of Surface Charge Density and Electrostatic Interaction. *Biophys. J.* **2006**, *90*, 1270−1274.
(18) Jackman, J. A.; Zan, G. H.; Zhao, Z.; Cho, N.-J. Contribution of the Hydration Force to Vesicle Adhesion on Titanium Oxide. *Langmuir* **2014**, *30*, 5368−5372.


DOI: 10.1021/am507651h
*ACS Appl. Mater. Interfaces* 2015, 7, 959−968

(19) Reimhult, E.; Höök, F.; Kasemo, B. Intact Vesicle Adsorption and Supported Biomembrane Formation from Vesicles in Solution: Influence of Surface Chemistry, Vesicle Size, Temperature, and Osmotic Pressure. *Langmuir* **2003**, *19*, 1681−1691.
(20) Jackman, J. A.; Cho, N.-J.; Duran, R. S.; Frank, C. W. Interfacial Binding Dynamics of Bee Venom Phospholipase A2 Investigated by Dynamic Light Scattering and Quartz Crystal Microbalance. *Langmuir* **2009**, *26*, 4103−4112.
(21) Gulcev, M. D.; Lucy, C. A. Factors Affecting the Behavior and Effectiveness of Phospholipid Bilayer Coatings for Capillary Electrophoretic Separations of Basic Proteins. *Anal. Chem.* **2008**, *80*, 1806−1812.
(22) Boudard, S.; Seantier, B.; Breffa, C.; Decher, G.; Felix, O. Controlling the Pathway of Formation of Supported Lipid Bilayers of DMPC by Varying the Sodium Chloride Concentration. *Thin Solid Films* **2006**, *495*, 246−251.
(23) Reimhult, E.; Höök, F.; Kasemo, B. Temperature Dependence of Formation of a Supported Phospholipid Bilayer from Vesicles on $SiO_2$. *Phys. Rev. E* **2002**, *66*, 051905.
(24) Cremer, P. S.; Boxer, S. G. Formation and Spreading of Lipid Bilayers on Planar Glass Supports. *J. Phys. Chem. B* **1999**, *103*, 2554−2559.
(25) Pfeiffer, I.; Zäch, M. Formation of Pit-Spanning Phospholipid Bilayers on Nanostructured Silicon Dioxide Surfaces for Studying Biological Membrane Events. In *Cellular and Subcellular Nanotechnology*; Weissig, V., Elbayoumi, T., Olsen, M., Eds.; Humana Press: New York, 2013; Chapter 12, pp 113−125.
(26) Reviakine, I.; Rossetti, F. F.; Morozov, A. N.; Textor, M. Investigating the Properties of Supported Vesicular Layers on Titanium Dioxide by Quartz Crystal Microbalance with Dissipation Measurements. *J. Chem. Phys.* **2005**, *122*, 204711.
(27) Richter, R. P.; Brisson, A. R. Following the Formation of Supported Lipid Bilayers on Mica: A Study Combining AFM, QCM-D, and Ellipsometry. *Biophys. J.* **2005**, *88*, 3422−3433.
(28) Groves, J. T.; Ulman, N.; Boxer, S. G. Micropatterning Fluid Lipid Bilayers on Solid Supports. *Science* **1997**, *275*, 651−653.
(29) Groves, J. T.; Ulman, N.; Cremer, P. S.; Boxer, S. G. Substrate-Membrane Interactions: Mechanisms for Imposing Patterns on a Fluid Bilayer Membrane. *Langmuir* **1998**, *14*, 3347−3350.
(30) Gun'ko, V.; Turov, V.; Zarko, V.; Voronin, E.; Tischenko, V.; Dudnik, V.; Pakhlov, E.; Chuiko, A. Active Site Nature of Pyrogenic Alumina/Silica and Water Bound to Surfaces. *Langmuir* **1997**, *13*, 1529−1544.
(31) Turov, V.; Leboda, R. Application of $^1$H NMR Spectroscopy Method for Determination of Characteristics of Thin Layers of Water Adsorbed on the Surface of Dispersed and Porous Adsorbents. *Adv. Colloid Interface Sci.* **1999**, *79*, 173−211.
(32) Tero, R.; Watanabe, H.; Urisu, T. Supported Phospholipid Bilayer Formation on Hydrophilicity-Controlled Silicon Dioxide Surfaces. *Phys. Chem. Chem. Phys.* **2006**, *8*, 3885−3894.
(33) Ahmed, S.; Madathingal, R. R.; Wunder, S. L.; Chen, Y.; Bothun, G. Hydration Repulsion Effects on the Formation of Supported Lipid Bilayers. *Soft Matter* **2011**, *7*, 1936−1947.
(34) Tero, R. Substrate Effects on the Formation Process, Structure and Physicochemical Properties of Supported Lipid Bilayers. *Materials* **2012**, *5*, 2658−2680.
(35) Berquand, A.; Mazeran, P.-E.; Pantigny, J.; Proux-Delrouyre, V.; Laval, J.-M.; Bourdillon, C. Two-Step Formation of Streptavidin-Supported Lipid Bilayers by PEG-Triggered Vesicle Fusion. Fluorescence and Atomic Force Microscopy Characterization. *Langmuir* **2003**, *19*, 1700−1707.
(36) Goh, H. Z.; Cho, N.-J. Rupture of Zwitterionic Lipid Vesicles by an Amphipathic, $\alpha$-Helical Peptide: Indirect Effects of Sensor Surface and Implications for Experimental Analysis. *Colloids Surf., B* **2014**, *121*, 340−346.
(37) Lazzara, T. D.; Kliesch, T.-T.; Janshoff, A.; Steinem, C. Orthogonal Functionalization of Nanoporous Substrates: Control of 3D Surface Functionality. *ACS Appl. Mater. Interfaces* **2011**, *3*, 1068−1076.
(38) Lazzara, T. D.; Carnarius, C.; Kocun, M.; Janshoff, A.; Steinem, C. Separating Attoliter-Sized Compartments Using Fluid Pore-Spanning Lipid Bilayers. *ACS Nano* **2011**, *5*, 6935−6944.
(39) Stephan, M.; Mey, I.; Steinem, C.; Janshoff, A. Combining Reflectometry and Fluorescence Microscopy: An Assay for the Investigation of Leakage Processes Across Lipid Membranes. *Anal. Chem.* **2014**, *86*, 1366−1371.
(40) Neubacher, H.; Mey, I.; Carnarius, C.; Lazzara, T. D.; Steinem, C. Permeabilization Assay for Antimicrobial Peptides Based on Pore-Spanning Lipid Membranes on Nanoporous Alumina. *Langmuir* **2014**, *30*, 4767−4774.
(41) Roskamp, R. F.; Vockenroth, I. K.; Eisenmenger, N.; Braunagel, J.; Köper, I. Functional Tethered Bilayer Lipid Membranes on Aluminum Oxide. *ChemPhysChem* **2008**, *9*, 1920−1924.
(42) Mager, M. D.; Almquist, B.; Melosh, N. A. Formation and Characterization of Fluid Lipid Bilayers on Alumina. *Langmuir* **2008**, *24*, 12734−12737.
(43) Venkatesan, B. M.; Polans, J.; Comer, J.; Sridhar, S.; Wendell, D.; Aksimentiev, A.; Bashir, R. Lipid Bilayer Coated $Al_2O_3$ Nanopore Sensors: Towards a Hybrid Biological Solid-State Nanopore. *Biomed. Microdevices* **2011**, *13*, 671−682.
(44) Kasprzyk-Hordern, B. Chemistry of Alumina, Reactions in Aqueous Solution and Its Application in Water Treatment. *Adv. Colloid Interface Sci.* **2004**, *110*, 19−48.
(45) Cho, N.-J.; Frank, C. W. Fabrication of a Planar Zwitterionic Lipid Bilayer on Titanium Oxide. *Langmuir* **2010**, *26*, 15706−15710.
(46) Cho, N.-J.; Jackman, J. A.; Liu, M.; Frank, C. W. pH-Driven Assembly of Various Supported Lipid Platforms: A Comparative Study on Silicon Oxide and Titanium Oxide. *Langmuir* **2011**, *27*, 3739−3748.
(47) Hohner, A. O.; David, M. P. C.; Rädler, J. O. Controlled Solvent-Exchange Deposition of Phospholipid Membranes onto Solid Surfaces. *Biointerphases* **2010**, *5*, 1−8.
(48) Tabaei, S. R.; Choi, J.-H.; Haw Zan, G.; Zhdanov, V. P.; Cho, N.-J. Solvent-Assisted Lipid Bilayer Formation on Silicon Dioxide and Gold. *Langmuir* **2014**, *30*, 10363−10373.
(49) Chen, M.; Li, M.; Brosseau, C. L.; Lipkowski, J. AFM Studies of the Effect of Temperature and Electric Field on the Structure of a DMPC−Cholesterol Bilayer Supported on a Au(111) Electrode Surface. *Langmuir* **2008**, *25*, 1028−1037.
(50) Marquês, J. T.; de Almeida, R. F.; Viana, A. S. Biomimetic Membrane Rafts Stably Supported on Unmodified Gold. *Soft Matter* **2012**, *8*, 2007−2016.
(51) Xu, S.; Szymanski, G.; Lipkowski, J. Self-Assembly of Phospholipid Molecules at a Au(111) Electrode Surface. *J. Am. Chem. Soc.* **2004**, *126*, 12276−12277.
(52) MacDonald, R. C.; MacDonald, R. I.; Menco, B. P. M.; Takeshita, K.; Subbarao, N. K.; Hu, L.-r. Small-Volume Extrusion Apparatus for Preparation of Large, Unilamellar Vesicles. *Biochim. Biophys. Acta, Biomembr.* **1991**, *1061*, 297−303.
(53) Rodahl, M.; Höök, F.; Fredriksson, C.; Keller, C. A.; Krozer, A.; Brzezinski, P.; Voinova, M.; Kasemo, B. Simultaneous Frequency and Dissipation Factor QCM Measurements of Biomolecular Adsorption and Cell Adhesion. *Faraday Discuss.* **1997**, *107*, 229−246.
(54) Voinova, M.; Jonson, M.; Kasemo, B. "Missing Mass" Effect in Biosensor's QCM Applications. *Biosens. Bioelectron.* **2002**, *17*, 835−841.
(55) Jonsson, P.; Jonsson, M. P.; Tegenfeldt, J. O.; Höök, F. A Method Improving the Accuracy of Fluorescence Recovery after Photobleaching Analysis. *Biophys. J.* **2008**, *95*, 5334−5348.
(56) Benes, M.; Billy, D.; Benda, A.; Speijer, H.; Hof, M.; Hermens, W. T. Surface-Dependent Transitions during Self-Assembly of Phospholipid Membranes on Mica, Silica, and Glass. *Langmuir* **2004**, *20*, 10129−10137.
(57) De Feijter, J. a.; Benjamins, J.; Veer, F. a. Ellipsometry as a Tool to Study the Adsorption Behavior of Synthetic and Biopolymers at the Air-Water Interface. *Biopolymers* **1978**, *17*, 1759−72.
(58) Sauerbrey, G. Verwendung von Schwingquarzen zur Wägung dünner Schichten und zur Mikrowägung. *Z. Phys.* **1959**, *155*, 206−222.


DOI: 10.1021/am507651h
*ACS Appl. Mater. Interfaces* 2015, 7, 959−968

(59) Kataoka-Hamai, C.; Inoue, H.; Miyahara, Y. Detection of Supported Lipid Bilayers Using Their Electric Charge. *Langmuir* **2008**, *24*, 9916−9920.
(60) Chiantia, S.; Ries, J.; Kahya, N.; Schwille, P. Combined AFM and Two-Focus SFCS Study of Raft-Exhibiting Model Membranes. *ChemPhysChem* **2006**, *7* (11), 2409−2418.
(61) Köchy, T.; Bayerl, T. M. Lateral Diffusion Coefficients of Phospholipids in Spherical Bilayers on a Solid Support Measured by $^{2}$H-Nuclear-Magnetic-Resonance Relaxation. *Phys. Rev. E* **1993**, *47* (3), 2109−2116.
(62) Kilpatrick, J. I.; Loh, S.-H.; Jarvis, S. P. Directly Probing the Effects of Ions on Hydration Forces at Interfaces. *J. Am. Chem. Soc.* **2013**, *135*, 2628−2634.
(63) Nabika, H.; Fukasawa, A.; Murakoshi, K. Tuning the Dynamics and Molecular Distribution of the Self-Spreading Lipid Bilayer. *Phys. Chem. Chem. Phys.* **2008**, *10*, 2243−2248.
(64) Jackman, J. A.; Choi, J.-H.; Zhdanov, V. P.; Cho, N.-J. Influence of Osmotic Pressure on Adhesion of Lipid Vesicles to Solid Supports. *Langmuir* **2013**, *29*, 11375−11384.
(65) Oleson, T. A.; Sahai, N. Interaction Energies between Oxide Surfaces and Multiple Phosphatidylcholine Bilayers from Extended-DLVO Theory. *J. Colloid Interface Sci.* **2010**, *352*, 316−326.
(66) Peng, P.-Y.; Chiang, P.-C.; Chao, L. Controllable Occurrence of Free-Standing Lipid Membranes on Nanograting Structured Supports. *ACS Appl. Mater. Interfaces* **2014**, *6*, 12261−12269.
(67) Israelachvili, J. N.; Pashley, R. M. Molecular Layering of Water at Surfaces and Origin of Repulsive Hydration Forces. *Nature* **1983**, *306*, 249−250.
(68) Israelachvili, J. N.; Wennerstroem, H. Hydration or Steric Forces between Amphiphilic Surfaces? *Langmuir* **1990**, *6*, 873−876.
(69) Cuddy, M. F.; Poda, A.; Brantley, L. N. Determination of Isoelectric Points and the Role of pH for Common Quartz Crystal Microbalance Sensors. *ACS Appl. Mater. Interfaces* **2013**, *5*, 3514−3518.
(70) Kosmulski, M. A Literature Survey of the Differences Between the Reported Isoelectric Points and Their Discussion. *Colloids Surf., A* **2003**, *222*, 113−118.


DOI: 10.1021/am507651h
*ACS Appl. Mater. Interfaces* 2015, 7, 959−968